Model of the Influence of an External Magnetic Field on the Gain of Terahertz Radiation from Semiconductor Superlattices

Timo Hyart,[1] Jussi Mattas,[1] and Kirill N. Alekseev[1,2]

[1]*Department of Physics, P. O. Box 3000, FI-90014 University of Oulu, Oulu, Finland*
[2]*Department of Physics, Loughborough University, Loughborough, LE11 3TU, United Kingdom*

(Received 24 June 2009; published 11 September 2009)

We theoretically analyze the influence of magnetic field on small-signal absorption and gain in a superlattice. We predict a very large and tunable THz gain due to nonlinear cyclotron oscillations in crossed electric and magnetic fields. In contrast to Bloch gain, here the superlattice is in an electrically stable state. We also find that THz Bloch gain can be significantly enhanced with a perpendicular magnetic field. If the magnetic field is tilted with respect to the superlattice axis, the usually unstable Bloch gain profile becomes stable in the vicinity of Stark-cyclotron resonances.

DOI: 10.1103/PhysRevLett.103.117401 PACS numbers: 78.67.De, 72.20.Ht, 73.21.Cd, 78.20.Ls

A semiconductor superlattice (SL) is a model system for a wealth of fundamental phenomena resulting from the wave-nature of charge carriers [1–3]. Interesting examples of such phenomena are Bloch oscillations in dc biased SLs [4], Shapiro-like steps [5] and parametric resonance [6] in time-dependent electric fields, coherent Hall effect in crossed electric and magnetic fields [7] and Stark-cyclotron resonances in tilted magnetic field [8]. The semiclassical theory predicts that electrons performing Bloch oscillations in the presence of weak dissipation can potentially provide THz Bloch gain [9]. The Bloch gain profile, which is shaped as a familiar dispersion curve, is not limited to SLs. It was recently predicted [10] and observed [11] in intersubband transitions of quantum cascade lasers, but dispersive gain profiles have been also found in the microwave responses of Josephson junctions [12] and Thim amplifiers [13]. Here we consider the Bloch gain in its traditional meaning as an effect occurring due to Bloch oscillations in a single energy band. In SLs, the realization of the Bloch oscillator is a long-standing problem due to the instability of a homogeneous electric field in conditions of negative differential conductivity (NDC) [14]. This electric instability results in a formation of electric domains in long SLs, which are destructive for the THz gain.

A considerable amount of theoretical and experimental activities have been devoted to the investigations of transient oscillations and voltage-current (VI) characteristics in the presence of magnetic field [2,7,8,15–18], but the response to a time-dependent field is mostly unexplored. In this Letter, we focus on the influence of the magnetic field on the small-signal absorption and gain. We find that absorption and gain profiles in crossed electric and magnetic fields have different characteristic shapes in the Bloch-like and cyclotronlike regimes of ballistic motion. We predict a very large and tunable THz gain due to nonlinear cyclotron oscillations in a single energy band. The cyclotron gain takes place in conditions of positive differential conductivity (PDC) and therefore it is stable against space-charge fluctuations. We also demonstrate that Bloch gain can be significantly enhanced by the perpendicular magnetic field. Moreover, the usually unstable Bloch gain profile becomes stable in the vicinity of Stark-cyclotron resonances if the magnetic field is tilted with respect to the SL axis.

We consider a SL under an action of a static magnetic field $\mathbf{B}$ in arbitrary direction and an electric field $E(t) = E_{\mathrm{dc}} + E_\omega \cos\omega t$ in a SL direction, which is chosen to be the x direction. Here $E_\omega \cos\omega t$ is a weak probe field with a frequency ω fixed by an external circuit (external cavity). We consider the electron transport in a single miniband with the standard tight-binding dispersion relation

$$\varepsilon(\mathbf{k}) = -(\Delta/2)\cos k_x d + \hbar^2(k_y^2 + k_z^2)/2m, \qquad (1)$$

where $\varepsilon(\mathbf{k})$ is the electron energy, $\mathbf{k}$ is its quasimomentum, Δ is the miniband width, d is the SL period, and m is the effective mass in y and z directions. We use the semiclassical approach based on the Boltzmann equation in the relaxation time τ approximation

$$\frac{\partial f}{\partial t} + \frac{1}{\hbar}[e\mathbf{E} + e\mathbf{v}\times\mathbf{B}]\cdot\frac{\partial f}{\partial \mathbf{k}} = -\frac{f - f_{\mathrm{eq}}}{\tau}, \qquad (2)$$

where $v_i(k_i) = \hbar^{-1}\partial\varepsilon(\mathbf{k})/\partial k_i$ $(i = x, y, z)$ are the velocity components and $f_{\mathrm{eq}}(\mathbf{k})$ is the Fermi distribution [2,3]. By solving Eq. (2), we find the stationary time-dependent current after transient

$$\mathbf{j}(t) = \frac{2e}{(2\pi)^3\tau}\int d^3k f_{\mathrm{eq}}(\mathbf{k})\int_{-\infty}^{t} ds\; e^{-(t-s)/\tau}\mathbf{v}(\mathbf{k}_s^t), \qquad (3)$$

where the prefactor takes into account the density of states [3], k_x is integrated over the Brillouin zone and the integration limits for k_y and k_z are $\pm\infty$. Here $\mathbf{k}_s^t$ is a ballistic trajectory governed by the equations

$$\frac{d\mathbf{k}_s^t}{dt} = \frac{1}{\hbar}[e\mathbf{E}(t) + e\mathbf{v}(\mathbf{k}_s^t)\times\mathbf{B}], \qquad \mathbf{k}_s^s = \mathbf{k}. \qquad (4)$$

The second equation in (4) means that the quasimomentum at $t = s$ is $\mathbf{k}$. We derived the solution of the Boltzmann equation (3) by using both a generalization of the technique based on the time-evolution operator [18] and the method of characteristics [19]. The approach based on this solution is most powerful in the limits of low carrier density N and low temperature. In this case

$$f_{\mathrm{eq}} \approx 4N\pi^3\delta(\mathbf{k}) \tag{5}$$

and the current (3) is determined by the ballistic trajectories starting at $\mathbf{k} = \mathbf{0}$.

The time-dependent current (3) can be used to calculate the real part of the dynamical conductivity $\sigma_r(\omega) \equiv \mathrm{Re}[\sigma(\omega)]$, which determines the gain ($\sigma_r < 0$) and absorption ($\sigma_r > 0$). In the absence of magnetic field σ_r is defined by the Tucker formula [3,20]

$$\sigma_r(\omega) = \frac{j_{\mathrm{dc}}(eE_{\mathrm{dc}}d + \hbar\omega) - j_{\mathrm{dc}}(eE_{\mathrm{dc}}d - \hbar\omega)}{2\hbar\omega} ed, \tag{6}$$

where $j_{\mathrm{dc}}(eE_{\mathrm{dc}}d)$ is the Esaki-Tsu characteristic [1],

$$j_{\mathrm{dc}}(eE_{\mathrm{dc}}d) = j_p \frac{2eE_{\mathrm{dc}}d\tau/\hbar}{1 + (eE_{\mathrm{dc}}d\tau/\hbar)^2}, \tag{7}$$

and j_p is the peak current corresponding to the critical field $E_{\mathrm{cr}} = \hbar/ed\tau$. The Drude conductivity of the SL is $\sigma_0 = 2j_p/E_{\mathrm{cr}}$. If $E_{\mathrm{dc}} > E_{\mathrm{cr}}$, Eq. (6) describes the dispersive Bloch gain profile [blue line in Fig. 3(b)] with a crossover from gain to loss at the resonance $\omega \approx \omega_B$, where $\omega_B = eE_{\mathrm{dc}}d/\hbar$ is the Bloch frequency. As directly follows from Eqs. (6) and (7), the upper limit for this Bloch gain is $\min[\sigma_r(\omega)] = -\sigma_0/8$.

We now turn to the consideration of electron dynamics in crossed electric and magnetic fields $\mathbf{B} = (0, 0, B_z)$. The ballistic electron dynamics under static fields is determined by the pendulum equation, which follows from Eq. (4) [2,15]. If the electrons start at the bottom of the miniband, the frequency of their nonlinear oscillations is

$$\Omega = \begin{cases} \pi\omega_c/2K(\omega_B/2\omega_c), & \omega_B < 2\omega_c \\ \pi\omega_B/2K(2\omega_c/\omega_B), & \omega_B > 2\omega_c, \end{cases} \tag{8}$$

where $\omega_c = eB_z/\sqrt{m_x m}$ and $m_x = 2\hbar^2/\Delta d^2$ are the cyclotron frequency and the effective mass at the bottom of the miniband, respectively. Here $K(k)$ is the complete elliptic integral of the first kind as a function of elliptic modulus. There exist two distinct regimes of motion: cyclotronlike oscillations for the large magnetic field $\omega_B < 2\omega_c$ (oscillations of pendulum) and Bloch-like oscillations for the dominating electric field $\omega_B > 2\omega_c$ (rotations of pendulum). As can be seen from Fig. 1(a), the frequency Ω is tunable by variation of the magnetic and electric fields. If $\omega_B \gg \omega_c$, we get from Eq. (8) that $\Omega = \omega_B$. In the opposite limit $\omega_B \ll \omega_c$ we have $\Omega = \omega_c$. Close to the separatrix $\omega_B = 2\omega_c$ oscillations are strongly nonlinear and anharmonic. All harmonics of Ω are present in the Bloch-like regime whereas only odd harmonics exist in the cyclotronlike regime. Such kind of transient oscillations have been directly observed in the experiments [7].

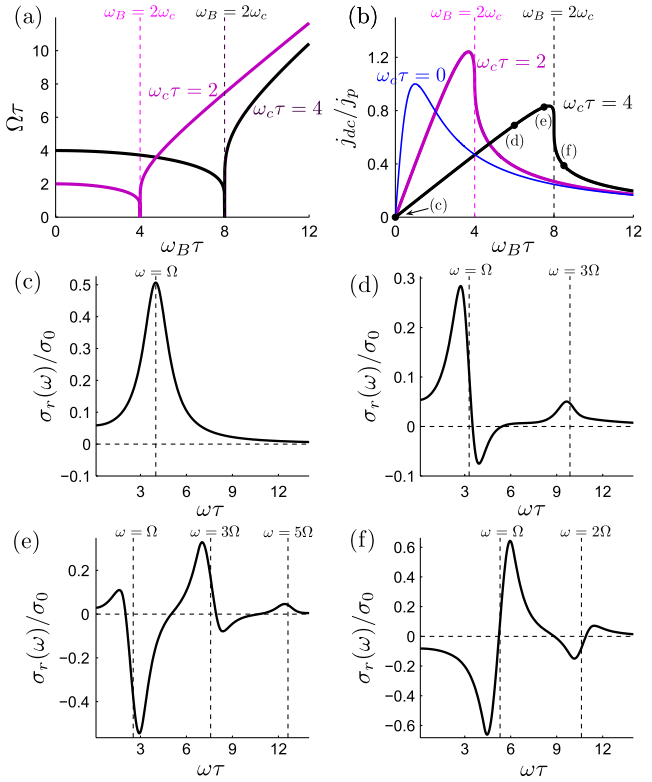

FIG. 1 (color online). (a) Frequency of the nonlinear oscillations Ω [Eq. (8)] as a function of ω_B for $\omega_c\tau =: 2, 4$. The dashed lines separate the cyclotronlike and Bloch-like regimes of motion. (b) VI characteristics for $\omega_c\tau =: 0, 2, 4$. (c)–(f) Absorption and gain profiles for $\omega_c\tau = 4$ and different values of electric field $\omega_B\tau =: 0$ (c), 6 (d), 7.5 (e) and 8.5 (f).

In the presence of scattering these oscillations determine the dc current density at low temperatures, as can be directly seen from Eqs. (3)–(5) [15]. The resulting VI characteristics for different values of the magnetic field are shown in Fig. 1(b). The transition from oscillatory to rotational motion at the separatrix $\omega_B = 2\omega_c$ manifests itself as a very abrupt and strong suppression of the dc current [15–17]. In the cyclotronlike regime, there are no Bragg reflections and therefore it corresponds the PDC part of the VI characteristic. On the other hand, the Bragg reflections in the Bloch-like regime result in NDC at the operation point. We find that the response of the miniband electrons to a weak ac field also shows clear signatures of the different types of ballistic motion. Figures 1(c)–1(f) show the absorption and gain profiles, calculated using Eqs. (3)–(5), for different values of ω_c and ω_B. The field strengths are chosen in such a way that the electrons perform several cycles of oscillations between the scattering events $\Omega\tau > 1$. We see that the gain and absorption profiles in the different regimes of oscillations have their own characteristic shapes. If $\omega_c \gg \omega_B$, electrons are restricted to the bottom of the miniband, and we obtain a

familiar Lorentzian absorption profile of a harmonic oscillator, which is centered at $\omega \approx \Omega$ [Fig. 1(c)]. In this case σ_r is always positive and an amplification of probe field is not possible. By increasing the electric field $E_{\rm dc}$ we obtain a completely different situation, where high-frequency gain can appear due to nonlinear cyclotron oscillations [Fig. 1(d) and 1(e)]. The characteristic shape of the gain profile turns out to be an inverse of the usual dispersive Bloch gain profile [cf. Figs. 1(d) and 2(b)]. In this gain profile the frequency of the nonlinear cyclotron oscillations Ω determines the position of a resonant crossover from loss to gain. When we are approaching the separatrix $\omega_B = 2\omega_c$, we see that replicas of this inverted dispersive gain profile appear at odd harmonics of Ω corresponding to the anharmonicity of the ballistic oscillations [Fig. 1(e)]. With a further increase of $E_{\rm dc}$ we reach the Bloch-like regime $\omega_B > 2\omega_c$. Here we always have a dispersive Bloch gain profile with a crossover frequency Ω [Fig. 1(f)]. Replicas of this gain profile can now appear at all harmonics of Ω.

Our results show that both the cyclotron gain and the Bloch-like gain have attractive properties such as tunability and extremely large magnitudes of the gain, which can be utilized in an operation of THz oscillators and amplifiers. The gain profiles in both regimes of motion are tunable by changing magnetic and electric fields. In the Bloch-like regime, the gain profile can be controlled more easily with a variation of the electric field, because Ω depends strongly on ω_B [see Fig. 1(a)]. In this regime Ω is sensitive to the magnetic field only near the separatrix. On the other hand, since the cyclotron gain exists only near the separatrix, it is tunable by simultaneous variation of the electric and magnetic fields as shown in Fig. 2(a). We see that large cyclotron gain can be obtained at frequencies $\omega\tau \geq 1$ if the cyclotron frequency is somewhat larger than the scattering rate $\omega_c\tau \geq 2$ [Fig. 2(a)]. In typical SLs $\tau \approx 200$ fs so that $\omega\tau = 1$ corresponds to the frequency $\omega/2\pi = 0.8$ THz. Therefore the cyclotron gain, similarly as the Bloch gain, is ideal for amplifiers and oscillators operating at THz frequencies.

We turn to the important issues of the magnitudes and the origin of the high-frequency gain. Figure 2(b) shows the Bloch gain profiles for fixed ω_B and different values of ω_c. We see that by increasing the magnetic field the gain

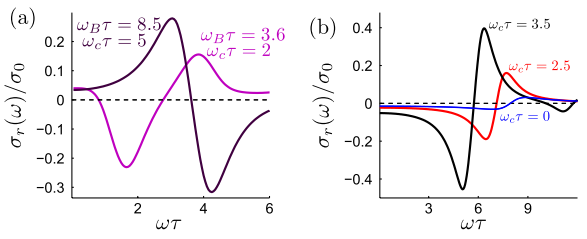

FIG. 2 (color online). (a) Cyclotron gain profiles for $\omega_B\tau = 3.6$, $\omega_c\tau = 2$ and $\omega_B\tau = 8.5$, $\omega_c\tau = 5$. (b) Bloch gain profiles for $\omega_B\tau = 8$ and different values of the magnetic field $\omega_c\tau =: 0$, 2.5, 3.5. The gain profiles were calculated using Eqs. (3)–(5).

increases roughly by an order of magnitude in comparison with the usual Bloch gain at $\mathbf{B} = \mathbf{0}$. Similarly, the THz cyclotron gain near the separatrix [Fig. 1(e)] is also an order of magnitude larger than the usual Bloch gain. For typical SL parameters $d = 6$ nm, $\Delta = 60$ meV, and $m = 0.067m_e$, we obtain that $\omega_c\tau = 1$ and $\omega_B\tau = 1$ correspond to the magnetic field $B = 2$ T and the electric field $E_{\rm dc} = 5.5$ kV/cm, respectively. Thus, already rather weak electric and magnetic fields can provide strong THz gain [Fig. 2(a)]. The magnitude of the gain α in units cm^{-1} is related to the dynamical conductivity as $\alpha = \alpha_0(\sigma_r/\sigma_0)$, where at low temperatures $\alpha_0 = Ne^2\tau/c\sqrt{\epsilon}\epsilon_0 m_x$. For moderate doping $N = 10^{16}$ cm^{-3} and relative permittivity $\varepsilon = 13$ (GaAs), we obtain $\alpha_0 \approx 833.5$ cm^{-1}. Using this value of α_0, it is easy to estimate all magnitudes of the gain in Figs. 1 and 2. In the vicinity of the separatrix, THz gain can have unprecedented values $\alpha \approx 500$ cm^{-1}.

Although the response to the ac field results from quite complicated nonlinear electron dynamics, we can identify an important role of the separatrix in the origin of this large THz gain. In the Bloch-like regime electrons periodically visit the upper part of the miniband and undergo Bragg reflections at the boundary of the Brillouin zone. In contrast there are no Bragg reflections in the cyclotronlike regime. However, a strong enough electric field $E_{\rm dc}$ periodically brings the carriers to the upper part of the miniband where their effective masses are negative [1,9]. We attribute the cyclotron gain to these nonclassical cyclotron oscillations in the presence of weak dissipation (scattering). As the electrons performing Bloch-like and cyclotronlike oscillations are spending more time in the upper part of the miniband the gain profiles become more pronounced. In the vicinity of the separatrix, the electron trajectories stick near the Brillouin zone boundary for a long time (the hyperbolic point of the pendulum) resulting in a significant enhancement of the THz gain [Figs. 1(e) and 2(b)].

Since in the cyclotronlike regime the SL operates in conditions of PDC, it is inherently stable with respect to the space-charge fluctuations. In the gain profiles this can be seen as positive dynamical conductivity at low frequencies [Figs. 1(c)–1(e) and 2(a)]. On the other hand, in the Bloch-like regime the gain always extends to the low frequencies [Figs. 1(f) and 2(b)] due to the operation in the NDC state [Fig. 1(b)]. This means that in the Bloch-like regime the problem of electric instability exists similarly as in the case of usual Bloch gain in SLs. Several different approaches have been suggested in order to stabilize the Bloch gain, including super-superlattice structures [21], quasistatic modulation of the bias [22] and 2D shunted surface SLs [17]. Here we demonstrate that the electric instability can be circumvented by introducing an additional magnetic field component in the SL direction, so that the magnetic field becomes tilted with respect to the SL axis $\mathbf{B} = (B_x, 0, B_z)$. In this case, electrons perform cyclo-

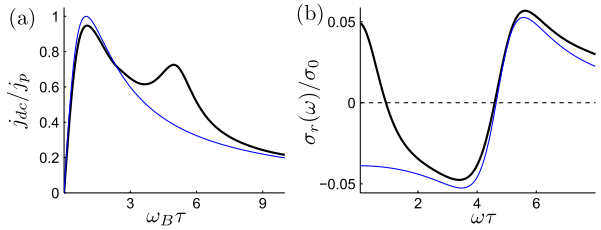

FIG. 3 (color online). (a) VI characteristic in tilted magnetic field, calculated using Eqs. (3)–(5), for $\omega_c\tau = 2$ and $\omega_{c\perp}\tau = 5$ (black line). The thin blue line shows the Esaki-Tsu VI characteristic [Eq. (7)]. (b) Gain profile for the same magnetic field and dc bias $\omega_B\tau = 4.75$ (black line). The thin blue line indicates the usual Bloch gain at $\mathbf{B} = \mathbf{0}$ [Eqs. (6) and (7)].

tron oscillations in the plane perpendicular to the SL axis with the frequency $\omega_{c\perp} = eB_x/m$. These in-plane cyclotron oscillations are coupled to the Bloch oscillations via the perpendicular magnetic field component ω_c. If ω_B and $\omega_{c\perp}$ are commensurate (Stark-cyclotron resonance), the coupling results in delocalization of the electrons, which reveals itself as additional resonant structures in the VI characteristics [8]. Figure 3(a) demonstrates such additional structure for a particular magnetic field. The enhancement of the current at the Stark-cyclotron resonance $\omega_B = \omega_{c\perp}$ resembles [23] the resonant structures in a VI characteristic induced by an auxiliary THz field [5]. By choosing the working point at the PDC part of the peak, we find, using Eqs. (3)–(5), that the gain profile close to the Bloch frequency $\omega \approx \omega_B$ has the usual shape of the dispersive Bloch gain, whereas the dynamical conductivity at low frequencies is now positive [Fig. 3(b)]. Interestingly, this stable gain profile can be well approximated by a variant of the Tucker formula (6), in which $j_{\mathrm{dc}}(eE_{\mathrm{dc}}d)$ is now the current density calculated in the presence of the magnetic field. We should distinguish our results from the recent proposal of sub-THz generation in SLs in tilted magnetic field [24]. There the moving charge domains are responsible for the current oscillations, whereas in our case the THz gain occurs in the absence of electric domains.

In summary, we found that the magnetic field significantly alters the shapes of gain profiles and the magnitude of THz gain in SLs. We described a novel type of large and tunable THz gain caused by nonlinear cyclotron oscillations in the crossed electric and magnetic fields. Since the operation point can be chosen at the PDC part of the VI characteristic the old problem of space-charge instability, which is typical for the Bloch gain in the SL, does not exist here. We also predicted an enhancement of the Bloch gain due to the nonlinear character of Bloch oscillations in the presence of a perpendicular magnetic field. Finally, we demonstrated that in the tilted magnetic field configuration the usual Bloch gain can be realized in conditions of PDC.

We conclude with two remarks. First, by numerically solving the Boltzmann equation (2), we observed that the cyclotron gain decreases rapidly with increasing temperature. It is typically smaller than the Bloch gain [3,10] already at 100 K. The stable THz gain in a tilted magnetic field, by contrast, declines slowly and has similar magnitudes as the usual Bloch gain also at room temperature. Secondly, the large-signal response near the separatrix can be quite different from the case of linear response. In the absence of scattering, the electron dynamics can even become chaotic. Nevertheless, we found that the cyclotron gain in conditions of PDC can still exist also for reasonably large amplitudes of the probe field $E_\omega > 2E_{\mathrm{cr}}$.

[1] L. Esaki and R. Tsu, IBM J. Res. Dev. **14**, 61 (1970).
[2] F. G. Bass and A. P. Tetervov, Phys. Rep. **140**, 237 (1986).
[3] A. Wacker, Phys. Rep. **357**, 1 (2002).
[4] J. Feldmann *et al.*, Phys. Rev. B **46**, 7252 (1992).
[5] K. Unterrainer *et al.*, Phys. Rev. Lett. **76**, 2973 (1996).
[6] T. Hyart, A. V. Shorokhov, and K. N. Alekseev, Phys. Rev. Lett. **98**, 220404 (2007).
[7] T. Bauer *et al.*, Phys. Rev. Lett. **88**, 086801 (2002); A. B. Hummel *et al.*, Phys. Status Solidi B **242**, 1175 (2005).
[8] F. G. Bass, V. V. Zorchenko, and V. I. Shashora, JETP Lett. **31**, 314 (1980); T. M. Fromhold *et al.*, Phys. Rev. Lett. **87**, 046803 (2001); Nature (London) **428**, 726 (2004); Yu. A. Kosevich *et al.*, Phys. Rev. Lett. **96**, 137403 (2006).
[9] S. A. Ktitorov, G. S. Simin, and V. Ya. Sindalovskii, Sov. Phys. Solid State **13**, 1872 (1972); A. A. Ignatov, K. F. Renk, and E. P. Dodin, Phys. Rev. Lett. **70**, 1996 (1993); H. Kroemer, arXiv:cond-mat/0007482v2.
[10] H. Willenberg, G. H. Döhler, and J. Faist, Phys. Rev. B **67**, 085315 (2003).
[11] R. Terazzi *et al.*, Nature Phys. **3**, 329 (2007).
[12] K. K. Likharev, *Dynamics of Josephson Junctions and Circuits* (Gordon and Breach, New York, 1986), Chap. 10, Chap. 11.
[13] H. W. Thim *et al.*, Appl. Phys. Lett. **7**, 167 (1965); D. E. McCumber and A. G. Chynoweth, IEEE Trans. Electron Devices **13**, 4 (1966).
[14] B. K. Ridley, Proc. Phys. Soc. London **82**, 954 (1963); A. A. Ignatov and V. I. Shashkin, Sov. Phys. JETP **66**, 526 (1987).
[15] V. M. Polyanovskii, Sov. Phys. Semicond. **14**, 718 (1980).
[16] A. Sibille *et al.*, Europhys. Lett. **13**, 279 (1990); J. F. Palmier *et al.*, Semicond. Sci. Technol. **7**, B283 (1992).
[17] T. Feil, C. Gerl, and W. Wegscheider, Phys. Rev. B **73**, 125301 (2006).
[18] F. G. Bass, V. V. Zorchenko, and V. I. Shashora, Sov. Phys. Semicond. **15**, 263 (1981).
[19] C. MacCallum, Phys. Rev. **132**, 930 (1963).
[20] J. R. Tucker, IEEE J. Quantum Electron. **15**, 1234 (1979).
[21] P. G. Savvidis *et al.*, Phys. Rev. Lett. **92**, 196802 (2004).
[22] T. Hyart *et al.*, Phys. Rev. Lett. **102**, 140405 (2009).
[23] T. Hyart, K. N. Alekseev, and E. V. Thuneberg, Phys. Rev. B **77**, 165330 (2008).
[24] M. T. Greenaway *et al.*, arXiv:0905.3717v1.